

## Supporting information

### **Two-Dimensional Functionalized Hexagonal Boron Nitride for Quantum Dot Photoelectrochemical Hydrogen Generation**

Omar Abdelkarim<sup>a</sup>, Jasneet Kaur<sup>b</sup>, Jiabin Liu<sup>a</sup>, Fabiola Navarro-Pardo<sup>a</sup>, Hadis Zarrin<sup>b</sup>, Aycan Yurtsever<sup>a</sup>,  
Ghada Bassioni<sup>c</sup>, Zhiming M. Wang<sup>d,e</sup>, Gurpreet Singh Selopal<sup>a,d\*</sup>, Federico Rosei<sup>a\*</sup>

<sup>a</sup> *Institut National de la Recherche Scientifique, Centre Énergie, Matériaux et Télécommunications, 1650 Boul.  
Lionel Boulet, Varennes, Québec, Canada J3X 1S2*

<sup>b</sup> *Department of Chemical Engineering, Faculty of Engineering & Architectural Science, Ryerson University,  
Toronto, Ontario M5B 2K3, Canada*

<sup>c</sup> *Ain Shams University, faculty of engineering, Chemistry Division, Cairo, Egypt P. O. Box 11517*

<sup>d</sup> *Institute of Fundamental and Frontier Sciences, University of Electronic Science and Technology of China,  
Chengdu 610054, PR China*

<sup>e</sup> *Institute of Micro Engineering and Nanoelectronic, Universiti Kebangsaan Malaysia, Bangi, 43600, Malaysia*

Email: [gurpreet.selopal@emt.inrs.ca](mailto:gurpreet.selopal@emt.inrs.ca); [rosei@emt.inrs.ca](mailto:rosei@emt.inrs.ca)

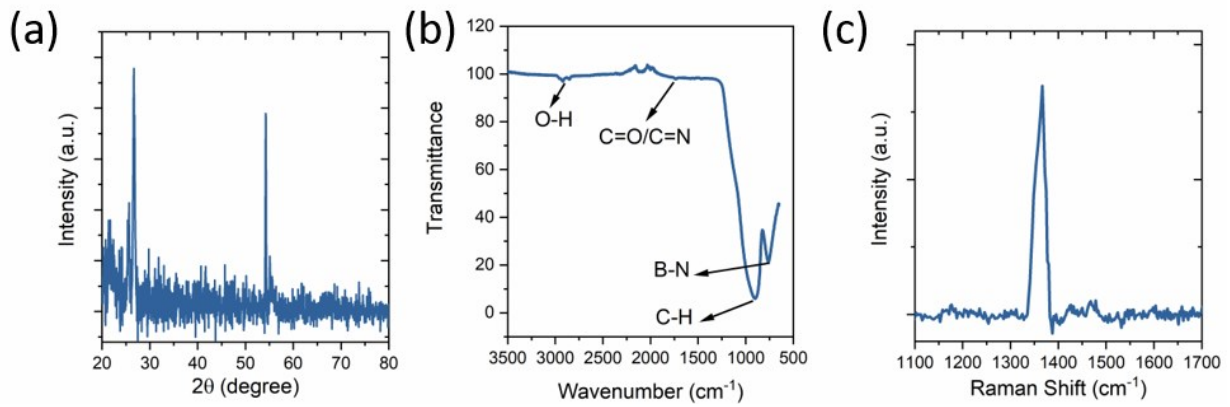


Figure S1 Structural characterizations of F-h-BN nanoflakes: (a) XRD; (b) FTIR; (c) Raman spectrum

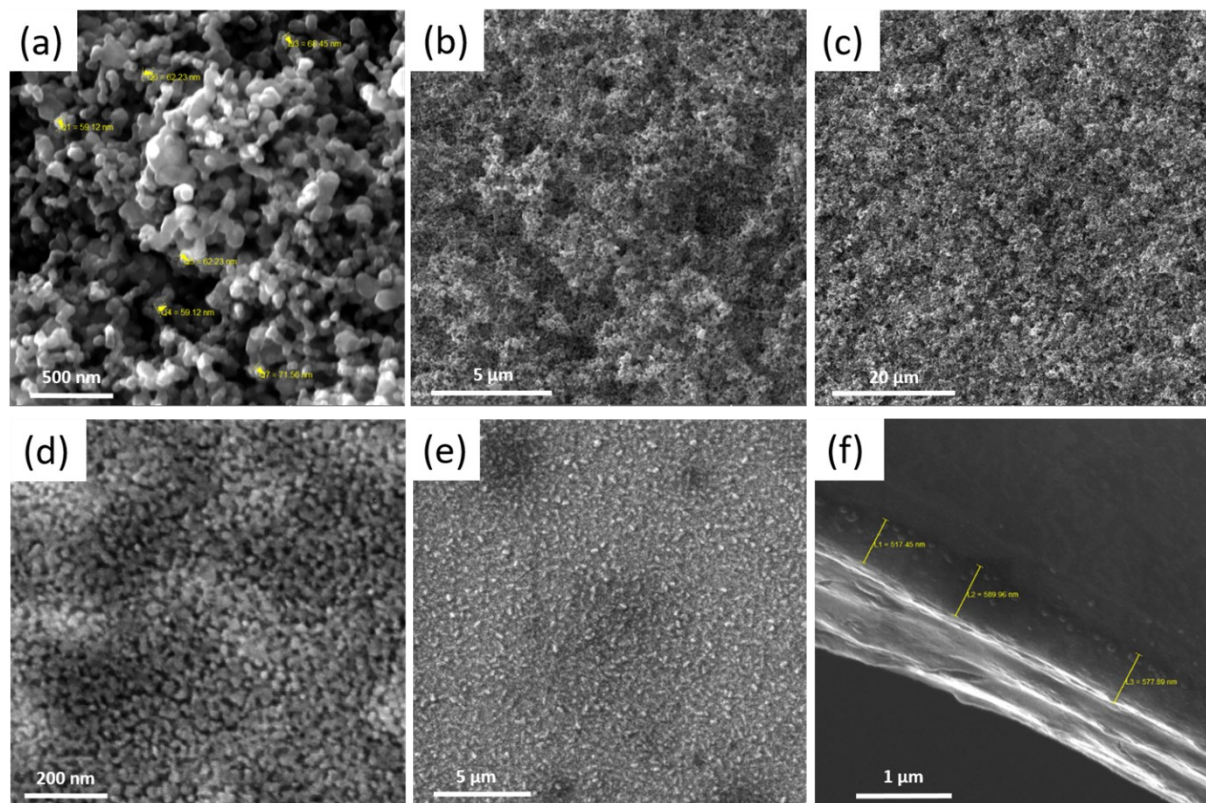


Figure S2 SEM images for (a) SnO<sub>2</sub> photoanode particle size (b) and (c) SnO<sub>2</sub> photoanode at lower magnification (d) and (e) SnO<sub>2</sub> blocking compact layer at high and low magnification (f) SnO<sub>2</sub> blocking layer thickness.

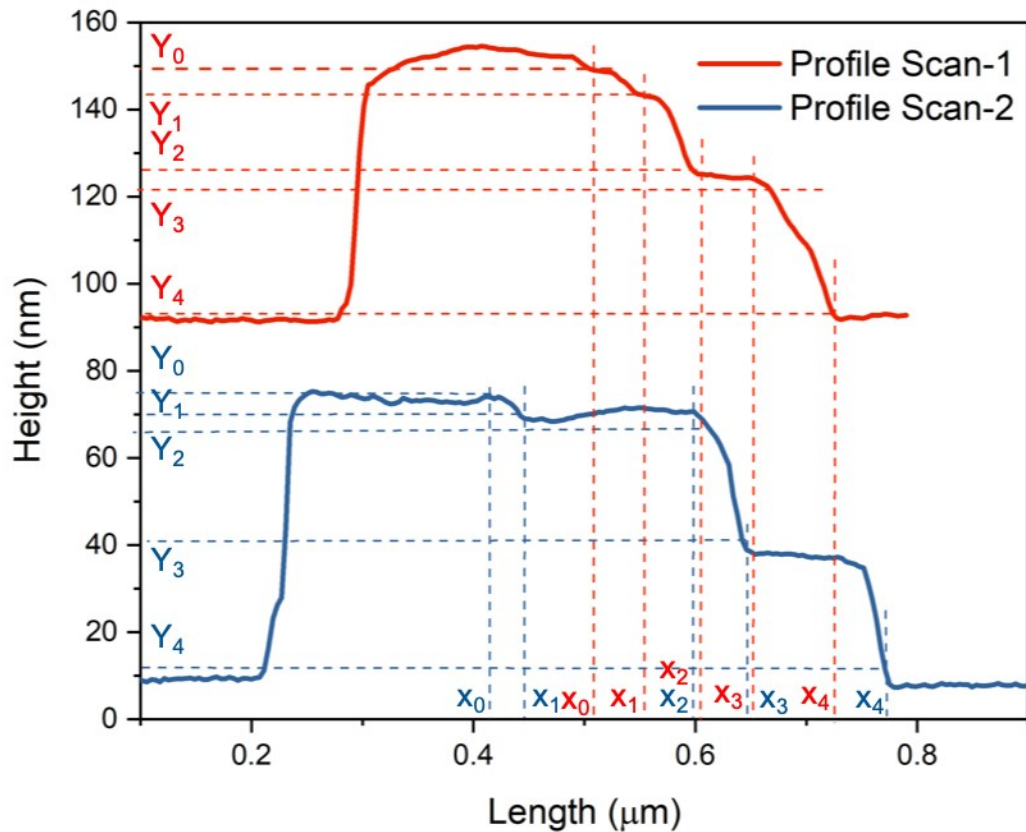


Figure S3 Thickness analysis of scanned F-h-BN nanoflakes: Profile 1 (red color line) and Profile 2 (Navy blue color line).

Table S1. Calculated thickness of F-h-BN nanoflakes from the AFM scan

Profile	Point $X_i$ ( $\mu\text{m}$ ) ( $i = 0 - 4$ )	$Y_j$ (nm) ( $j = 0 - 4$ )	Length (nm)	Thickness (nm)	Angle (deg)
Profile-1	0.419	57.2			
	0.465	52.3	45	4.9	-6.14
	0.594	54.1	130	1.8	0.80
	0.657	21.6	63	32.6 (3-4 layers)	-27.53
	0.788	-8.8	131	30.3 (3-4 layers)	-13.03
Profile-2	0.484	53.5			
	0.514	50.2	29	3.3	-6.36
	0.554	44.6	41	5.6	-7.86
	0.606	26.6	52	18.1 (2-3 layers)	-19.16
	0.739	-6.3	133	32.9 (3-4 layers)	-13.94

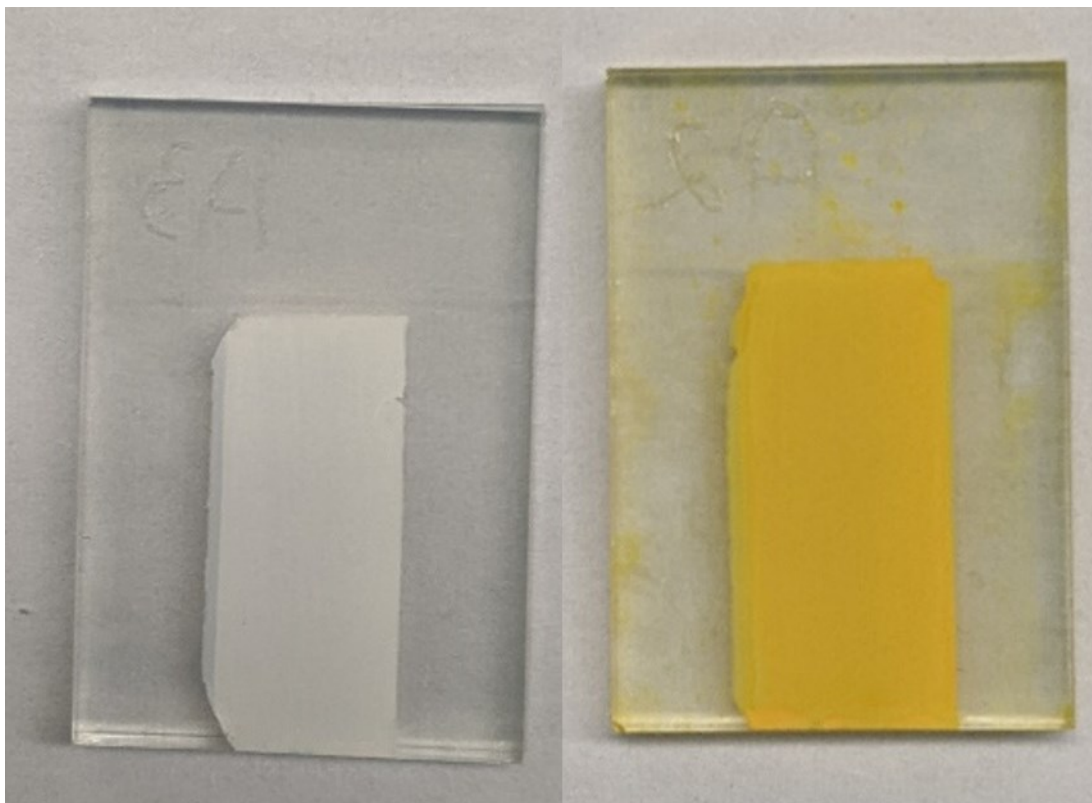


Figure S4 Visual inspection for  $\text{SnO}_2/\text{TiO}_2/\text{F-h-BN}$  photoanode before and after sensitization with CdS QDs using 7 cycles of SILAR method.

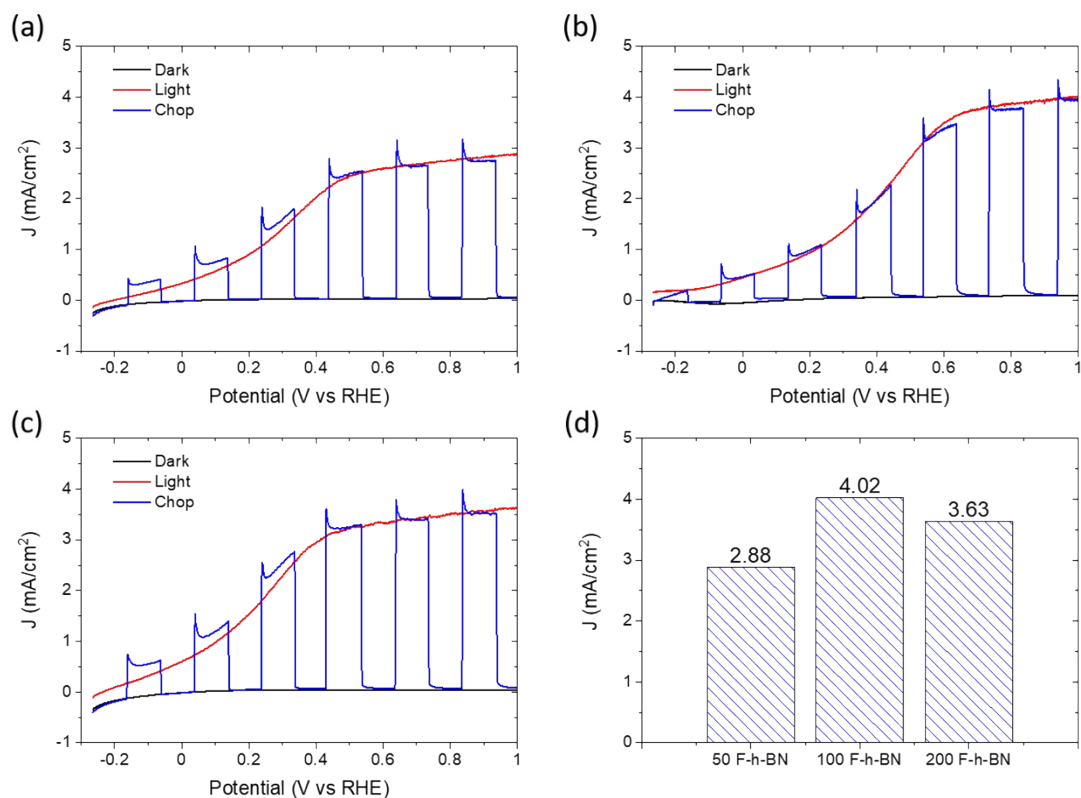


Figure S5 PEC performance under dark, light and chop for two-layer SnO<sub>2</sub>/F-h-BN/CdS photoanode with different amounts of F-h-BN solution: (a) 50 μl; (b) 100 μl; (c) 200 μl. (d) Comparison of the saturated photocurrent density at 1.0 V vs RHE with different amounts of F-h-BN solution.

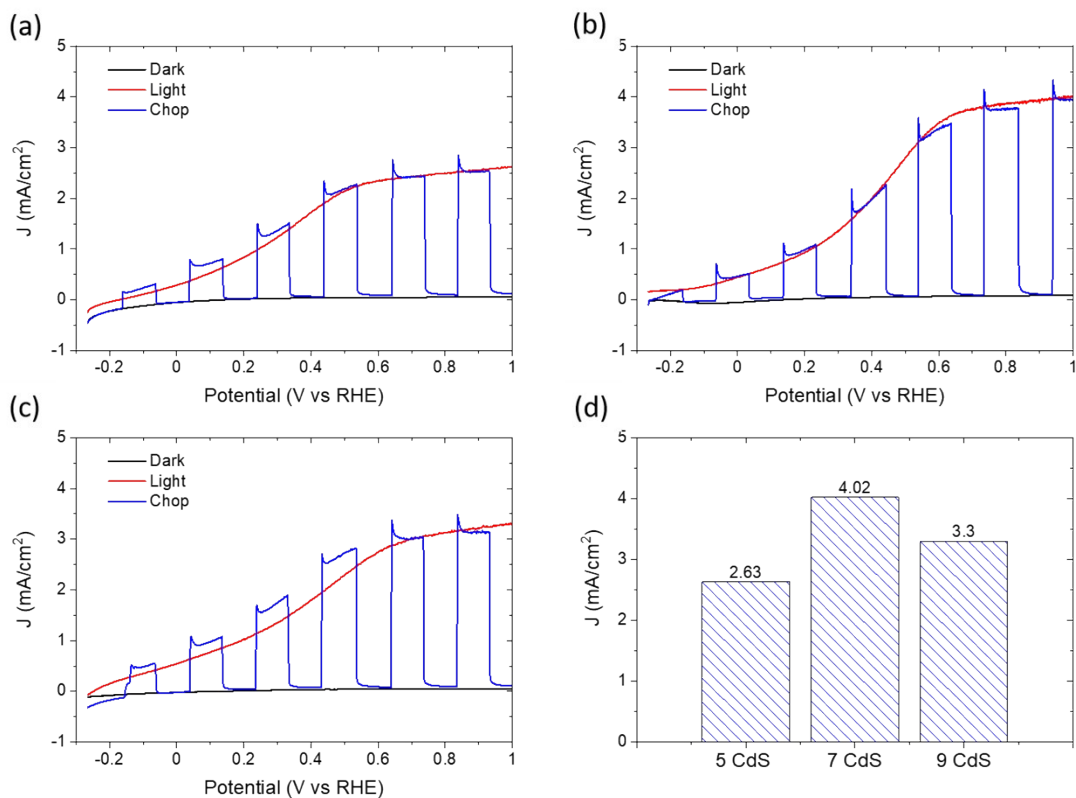


Figure S6 PEC performance under for two-layer SnO<sub>2</sub>/100 μl F-h-BN/CdS photoanode with different numbers of CdS QDs SILAR cycles: (a) 5; (b) 7; (c) 9. (d) Comparison of the saturated photocurrent density at 1.0 V vs RHE with different numbers of CdS QDs SILAR cycles.

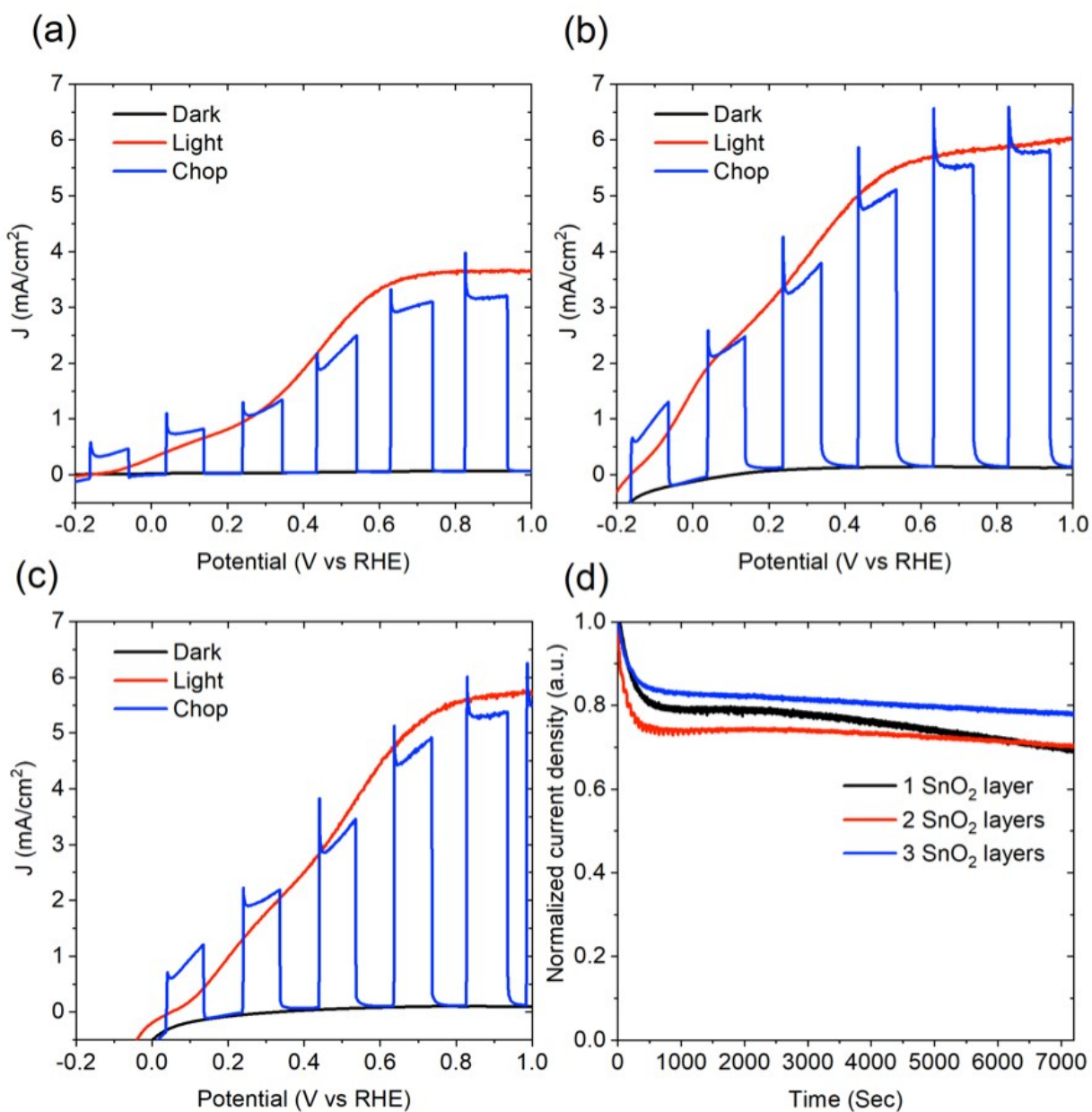


Figure S7 PEC performance under dark, light, and chop for SnO<sub>2</sub>/F-h-BN/CdS/CdSe/ZnS photoanode with a different number of SnO<sub>2</sub> mesoporous film layers: (a) One layer; (b) Two layers; (c) Three layers of SnO<sub>2</sub>. (d) Stability performance: Normalized current density vs time (sec).

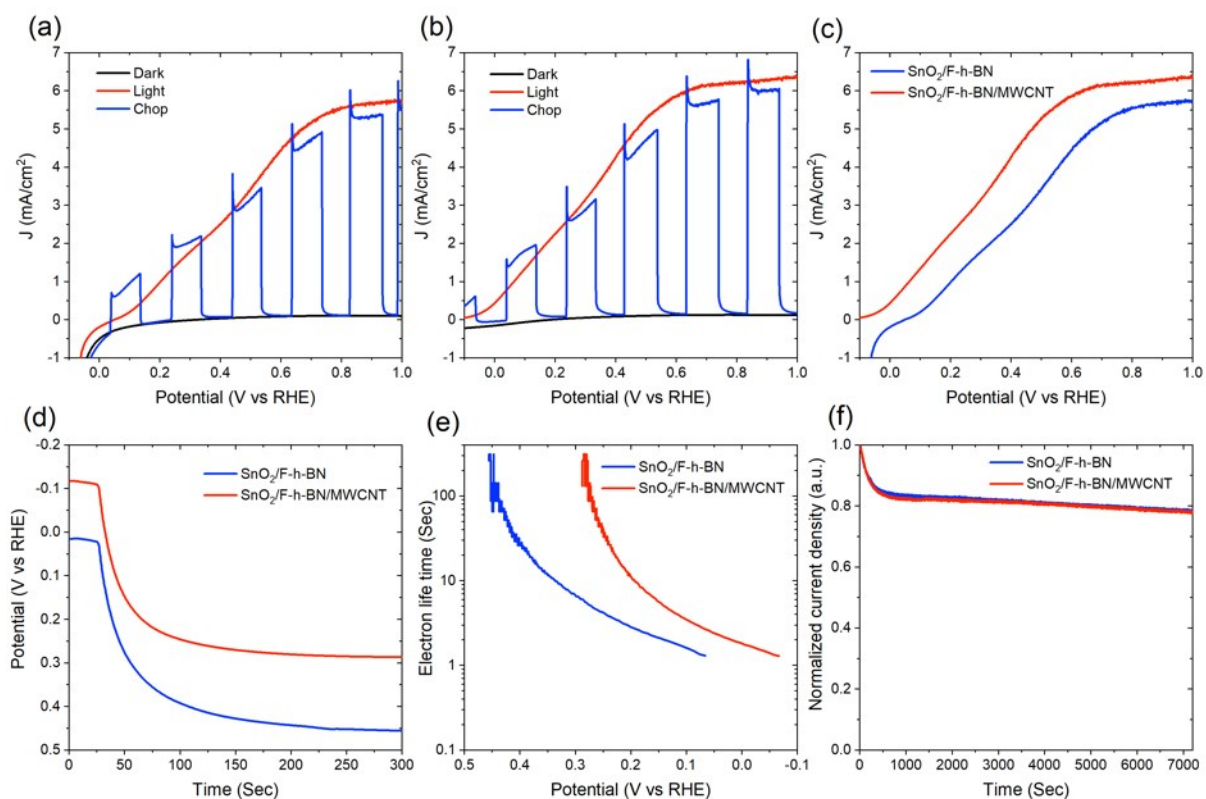


Figure S8 PEC performance under dark, light and chop for three layers SnO<sub>2</sub>/CdS/CdSe/ZnS photoanode: (a) with F-h-BN; (b) with F-h-BN and MWCNTs; (c) Comparison of photocurrent density vs potential (V vs RHE) for PEC devices based on F-h-BN and F-h-BN/MWCNT under continuous illumination. (d) Open circuit voltage. (e) Electron lifetime. and (f) Stability performance: Normalized current density vs time (sec).

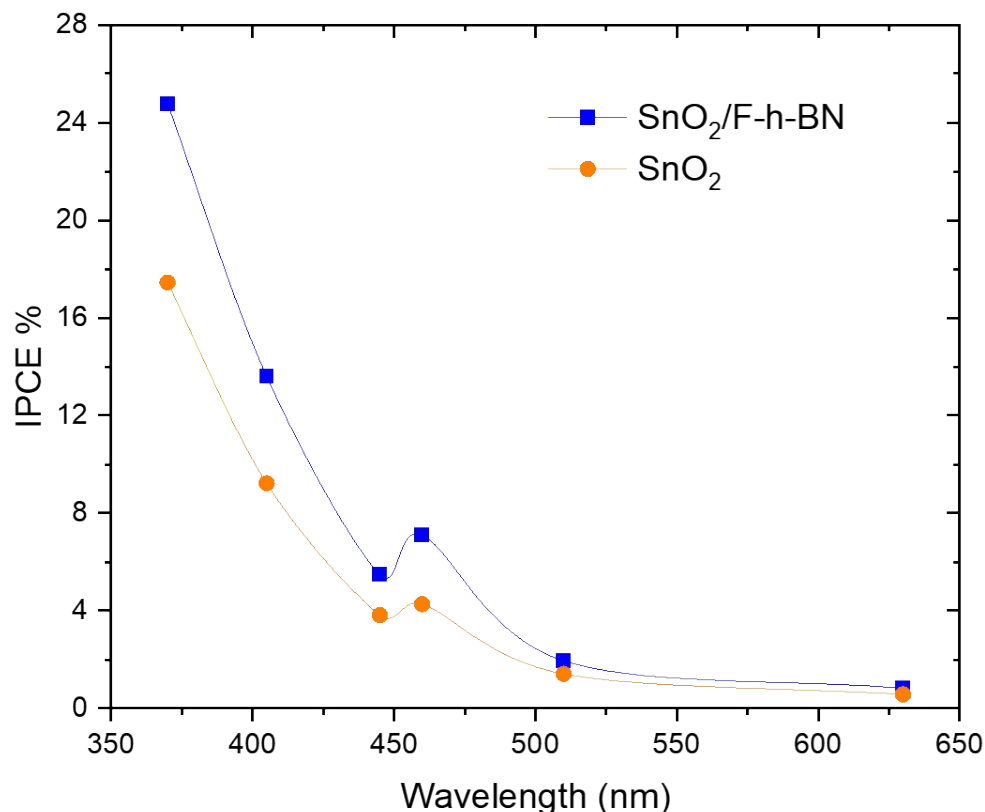


Figure S9 IPCE measurement for PEC device based on SnO<sub>2</sub> mesoporous film, with and without F-h-BN, sensitized with CdS/CdSe QDs.

We observe significant differences between the photocurrent density values measured from the J-V curves and the those calculated from the IPCE data. The photocurrent density values from J-V measurements are 6.05 mA.cm<sup>-2</sup> and 5.4 mA.cm<sup>-2</sup>, whereas the values obtained from the IPCE measurements are 1.53 mA.cm<sup>-2</sup> and 1.04 mA.cm<sup>-2</sup> for SnO<sub>2</sub>/F-h-BN and SnO<sub>2</sub>, respectively. The significant differences between photocurrent density values obtained from J-V measurements as opposed to values calculated from IPCE data, is due to the experimental procedures we adopted for the IPCE measurements. For instance, in this specific case, we used a manual system for the IPCE measurement by placing optical filters of different wavelengths in front of the solar simulator to obtain monochromatic light. The overall light intensity obtained through these optical filters may be lower compared to the intensity of the monochromatic light source (built in the IPCE system). In addition, the light intensity is different between the monochromatic optical filter measured using a reference cell and the PEC measurement cell. The number of photons is also not equivalent due to the difference in the refractive index of the materials and electrolyte used in the PEC device. Further, the illumination area is smaller in the IPCE measurement than that in the J-V measurement. When the illuminated area is limited, a

larger number of micro shunt resistances are present (acting as recombination centers) that reduce the photogenerated current density values obtained from the IPCE measurements.

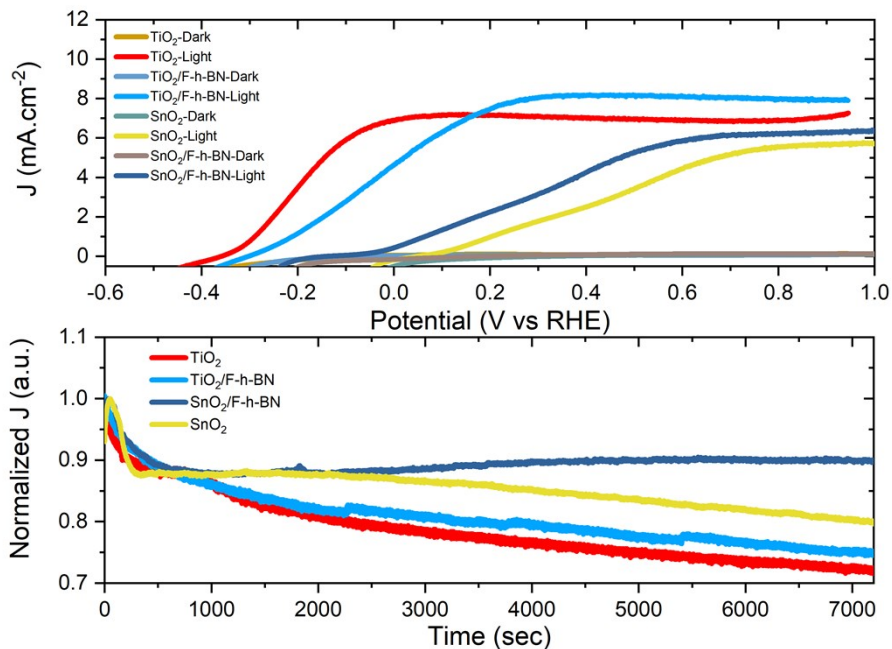


Figure S10. PEC performance comparison between SnO<sub>2</sub>/CdS/CdSe/ZnS and TiO<sub>2</sub>/CdS/CdSe/ZnS with and without F-h-BN photoanode: (a) dark and light performance of the photoanodes. (b) Stability performance of the corresponding PEC devices: Normalized saturated photocurrent density vs time (sec).

### The calculation process for the band structure in Figure S11:

From the UPS measurement in Figure S11 (d), we can obtain the valence band offset and work function, from Figure S11 (c) and (e), respectively.

The ionization potential (IP), which is the difference between the vacuum level and valence band maximum (VBM), can be calculated by adding the (valence band offset) to the (21.22 eV “Helium source energy” work function)

- In the case of SnO<sub>2</sub>, the IP = 4.04 + (21.22 – 17.12) = 8.14 eV, therefore the VBM of SnO<sub>2</sub> is -8.14 eV vs. vacuum.
- In the case of SnO<sub>2</sub>/F-h-BN, the IP = 4.06 + (21.22 – 16.74) = 8.54 eV, therefore VBM of SnO<sub>2</sub>/F-h-BN is -8.54 eV vs. vacuum.

To calculate the conduction band minimum (CBM) we added the optical band gap obtained from UV-Vis measurements, in Figure S11 (a) to the VBM.

- In case of SnO<sub>2</sub>, The CBM = -8.14 + 3.80 = - 4.34 eV vs Vacuum
- In case of SnO<sub>2</sub>/F-h-BN, The CBM = -8.54 + 3.89 = - 4.65 eV vs Vacuum

To change the values from Vacuum to SHE, we use this equation:  $SHE = -(\text{Vacuum} + 4.5)$

- For  $\text{SnO}_2$  {VBM =  $-(-8.14 + 4.5) = 3.64$  eV | CMB =  $-(-4.34 + 4.5) = -0.16$  eV Vs SHE}
- For  $\text{SnO}_2/\text{F-h-BN}$  {VBM =  $-(-8.54 + 4.5) = 4.04$  eV | CBM =  $-(-4.65 + 4.5) = 0.15$  eV Vs SHE}

To change the values from SHE to RHE, we use the following equation:  $RHE = SHE - (0.059 \cdot \text{pH})$

- For  $\text{SnO}_2$  {VBM =  $3.64 - (0.059 \cdot 13) = 2.87$  eV | CMB =  $-0.16 - (0.059 \cdot 13) = -0.92$  eV vs RHE}
- For  $\text{SnO}_2/\text{F-h-BN}$  {VBM =  $4.04 - (0.059 \cdot 13) = 3.27$  eV | CBM =  $0.15 - (0.059 \cdot 13) = -0.61$  eV Vs RHE}

The HER and OER calculations

- HER =  $0 - (0.059 \cdot 13) = -0.767$  eV
- OER =  $1.23 - (0.059 \cdot 13) = 0.463$  eV

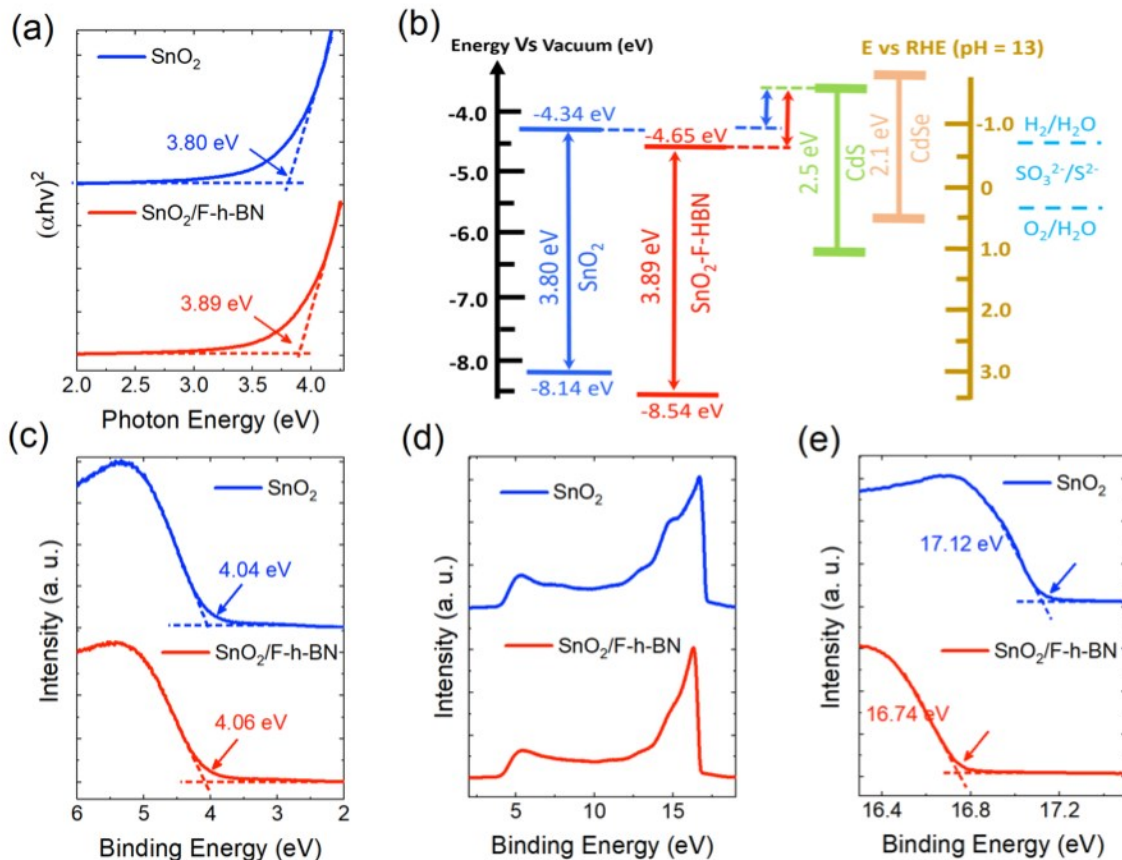


Figure S11 Band alignment of  $\text{SnO}_2$  and  $\text{SnO}_2/\text{F-h-BN}$ : (a) measured band gaps of  $\text{SnO}_2$  and  $\text{SnO}_2/\text{F-h-BN}$  (b) schematic of the overall band structure of  $\text{SnO}_2$  and  $\text{SnO}_2/\text{F-h-BN}$  with respect

to CdS-CdSe QDs; UPS measurement of SnO<sub>2</sub> and SnO<sub>2</sub>/F-h-BN: (c) Fermi level estimation; (d) Full spectra; (e) VBM estimation.

Table S2 EIS measurement under the dark condition for SnO<sub>2</sub> and SnO<sub>2</sub>/F-h-BN

Data	SnO <sub>2</sub>	SnO <sub>2</sub> /F-H-BN	Unit
R1	15.2	12.5	Ohm
R2	$5.23 \times 10^5$	$3.00 \times 10^5$	Ohm
R3	25203	$5.40 \times 10^5$	Ohm
C2	$4.53 \times 10^{-5}$	$8.19 \times 10^{-6}$	F
C3	$3.64 \times 10^{-6}$	$1.75 \times 10^{-5}$	F
Ws1-R	63142	$1.42 \times 10^5$	Ohm
Ws1-T	1.649	5.5	Sec
The constant phase elements used to calculate the capacitance			
CPE1-T	$3.33 \times 10^{-5}$	$7.04 \times 10^{-6}$	Q
CPE1-P	0.90293	0.832	n
CPE2-T	$4.03 \times 10^{-6}$	$1.50 \times 10^{-5}$	Q
CPE2-P	0.958	0.932	n

Table S3 Onset potential values for different PEC devices

PEC Device	Potential (V vs Ag/AgCl)
SnO <sub>2</sub> /CdS	0.36
SnO <sub>2</sub> /F-h-BN/CdS	0.33
SnO <sub>2</sub> /CdS/CdSe	0.29
SnO <sub>2</sub> /F-h-BN/CdS/CdSe	0.12